JOURNAL OF THEORETICAL
AND APPLIED MECHANICS
1, **38**, 2000

MATHEMATICAL MODEL OF UAV IN NUMERICAL SIMULATION OF THE RECOVERY MANOEUVRE IN A PERTURBED FLIGHT

MARIUSZ KRAWCZYK
JERZY GRAFFSTEIN
JERZY MARYNIAK

Institute of Aviation, Warsaw
e-mail: krawczyk@ilot.edu.pl, jgraff@ilot.edu.pl

The study presents a mathematical model in terms of the Boltzmann-Hamel equations representing a controlled Unmanned Aerial Vehicle (UAV) motion. The widely known problems with takeoff and recovery manoeuvres of UAV are considered. Both manoeuvres are characterised by low velocities, large angles of attack and relatively low efficiency of the control, so the sophisticated procedures are then necessary to ensure flight safe during these phases of motion. Some results of the first phase of recovery manoeuvre numerical simulations are reported.

Key words: aerospace dynamic and control, inverse simulation, control system design, UAV

1. Introduction

For the last two decades of the twentieth century we have observed intensive development of the reconnaissance methods, in which the Unmanned Aerial Vehicles (UAVs) are employed in completing of both pseudo- and fully autonomous missions. Application of the UAV affects substantially the mission planning requirements (Blajer, 1995; Blajer et al., 1997; Graffstein and Krawczyk, 1996; Graffstein et al., 1998).

Generally, the UAV mission consists of certain phases:

- Flight along a straight line (approximately)

- More complex flight trajectory when executing complicated manoeuvres; namely, take off, recovery, circulation over way point, terrain searching, etc. (Blajer, 1995; Graffstein et al., 1998).

The paper deals with the UAV recovery manoeuvre. As a test object it was used the UAV "SOWA", for which a mathematical model was built.

2. General model of UAV dynamics

The UAV is controlled by deflections of the control surfaces: elevator δ_H, rudder δ_V, aileron δ_L and the thrust value changes T as a function of the throttle deflection δ_T.

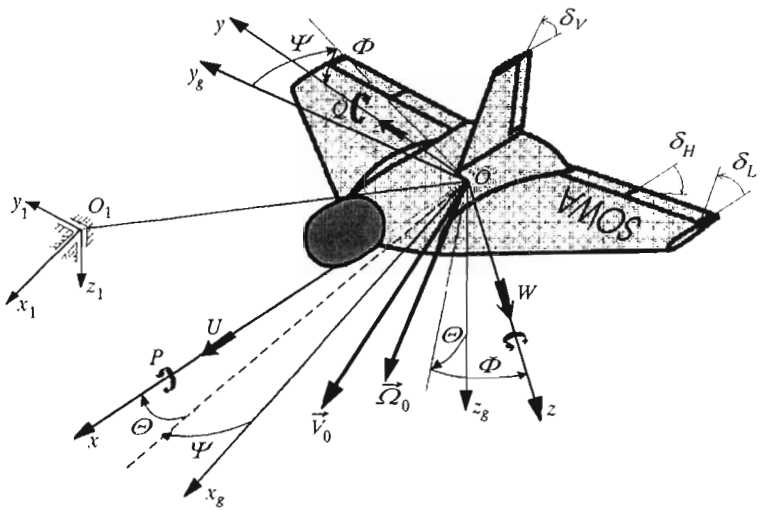

Fig. 1. Co-ordinate systems

The physical model of UAV dynamics represents also the influence of control surfaces mass centre displacement relative to its own axis of rotation. In the mathematical model of UAV dynamics derived within the framework of Boltzmann-Hamel formalism (Graffstein et al., 1997; Maryniak, 1992), it is represented as a mechanical system in the body-fixed axes $Oxyz$ (Fig.1) with the holonomic constraints

$$\frac{d}{dt}\frac{\partial T^*}{\partial \omega_\mu} - \frac{\partial T^*}{\partial \pi_\mu} + \sum_{r=1}^{k}\sum_{\alpha=1}^{l}\gamma^r_{\mu\alpha}\frac{\partial T^*}{\partial \omega_r}\omega_\alpha = Q^*_\mu \qquad \alpha,\mu,r = 1,2,...,k \tag{2.1}$$

where

k – number of degrees of freedom
ω_μ – quasi-velocity
T^* – kinetic energy
π_μ – quasi-coordinates
Q^*_μ – generalized forces
$\gamma^r_{\alpha\mu}$ – Boltzmann coefficient.

Let us introduce the following generalised co-ordinate vector $\boldsymbol{q}$ and quasi-velocity vector $\boldsymbol{\omega}$

$$\begin{aligned} \boldsymbol{q} &= [x_1, y_1, z_1, \Phi, \Theta, \Psi, \delta_H, \delta_V, \delta_L]^\top \\ \boldsymbol{\omega} &= [U, V, W, P, Q, R, \omega_7, \omega_8, \omega_9]^\top \end{aligned} \tag{2.2}$$

where ω_7, ω_8, ω_9 are

$$\begin{aligned} \omega_7 &= K^H_\Theta(\Theta - \Theta_z) + K^H_Q(Q - Q_z) + K^H_W(W - W_z) + K^H_x(x_1 - x_{1z}) + \\ &+ K^H_z(z_1 - z_{1z}) + K^H_U(U - U_z) + \delta_{H0} - T^H_2\delta_H \\ \omega_8 &= K^V_\Phi(\Phi - \Phi_z) + K^V_P(P - P_z) + K^V_W(W - W_z) + K^V_y(y_1 - y_{1z}) + \\ &+ K^V_V(V - V_z) + K^V_\psi(\Psi - \Psi_z) + K^V_R(R - R_z) + \delta_{V0} - T^V_2\delta_V \\ \omega_9 &= K^L_\Phi(\Phi - \Phi_z) + K^L_P(P - P_z) + K^L_W(W - W_z) + K^L_y(y_1 - y_{1z}) + \\ &+ K^L_V(V - V_z) + K^L_\psi(\Psi - \Psi_z) + K^L_R(R - R_z) + \delta_{L0} - T^L_2\delta_L \end{aligned} \tag{2.3}$$

respectively (Graffstein et al., 1997), and the throttle deflection is defined as follows

$$\begin{aligned} &T^T_3\dot{\delta}_T + T^V_2\delta_T = K^T_\Theta(\Theta - \Theta_z) + K^T_Q(Q - Q_z) + K^T_U(U - U_z) + \\ &+K^T_W(W - W_z) + K^T_z(z_1 - z_{1z}) + K^T_\Phi(\Phi - \Phi_z) + K^T_\Psi(\Psi - \Psi_z) + \delta_{T0} \end{aligned} \tag{2.4}$$

where K^j_i and T^j_i are the gains and time constants, respectively.

The non-zero Boltzmann coefficients (Maryniak, 1992) in the energetic equations of UAV motion were calculated on the assumption that energy of the plane T^* is a sum of UAV and all control surfaces energy, yielding nine differential equations of motion in the form (Graffstein et al., 1997; Maryniak, 1992)

$$\mathbf{M}\dot{\boldsymbol{V}} + \mathbf{K}\mathbf{M}_1\boldsymbol{V} + \mathbf{K}_s\boldsymbol{V} + \mathbf{K}_{wz}\boldsymbol{H} = \boldsymbol{Q} \tag{2.5}$$

where

$\mathbf{M}, \mathbf{M}_1$ – matrices of mass
$\mathbf{K}$ – matrix of inertia
$\mathbf{M}_s$ – velocity matrix
$\boldsymbol{Q}$ – vector of aerodynamic and gravitational forces

$$\mathbf{M}=\begin{bmatrix} m & 0 & 0 & 0 & S_z^1 & -S_y^1 & 2S_{H1} & -S_{V1} & 0 \\ 0 & m & 0 & -S_z^1 & 0 & S_x^1 & 0 & S_{V2} & 0 \\ 0 & 0 & m & S_y^1 & -S_x^1 & 0 & -2S_{H2} & 0 & 0 \\ 0 & -S_z^1 & S_y^1 & J_x^1 & -J_{xy}^1 & -J_{xz}^1 & 0 & -J_{V1} & -2J_{L1} \\ S_z^1 & 0 & -S_x^1 & -J_{xy}^1 & J_y^1 & -J_{yz}^1 & 2J_{yH}^1 & -J_{V2} & 0 \\ -S_y^1 & S_x^1 & 0 & -J_{xz}^1 & -J_{yz}^1 & J_z^1 & 0 & J_{zV}^1 & -2J_{L3} \\ S_{H1} & 0 & -S_{H2} & -J_{H1} & J_{yH}^1 & -J_{H3} & J_{yH}^1 & 0 & 0 \\ -S_{V1} & S_{V2} & 0 & -J_{V1} & J_{V2} & J_{zV}^1 & 0 & J_{zV}^1 & 0 \\ S_{L1} & 0 & -S_{L2} & -J_{L1} & J_{yL}^1 & -J_{L3} & 0 & 0 & J_{yL}^1 \end{bmatrix}$$

$$\mathbf{M}_1=\begin{bmatrix} m & 0 & 0 & 0 & S_z^1 & -S_y^1 & 0 & 0 & 0 \\ 0 & m & 0 & -S_z^1 & 0 & S_x^1 & 0 & 0 & 0 \\ 0 & 0 & m & S_y^1 & -S_x^1 & 0 & 0 & 0 & 0 \\ 0 & -S_z^1 & S_y^1 & J_x^1 & -J_{xy}^1 & -J_{xz}^1 & 0 & 0 & 0 \\ S_z^1 & 0 & -S_x^1 & -J_{xy}^1 & J_y^1 & -J_{yz}^1 & 0 & 0 & 0 \\ -S_y^1 & S_x^1 & 0 & -J_{xz}^1 & -J_{yz}^1 & J_z^1 & 0 & 0 & 0 \\ 0 & 0 & 0 & 0 & 0 & 0 & 0 & 0 & 0 \\ 0 & 0 & 0 & 0 & 0 & 0 & 0 & 0 & 0 \\ 0 & 0 & 0 & 0 & 0 & 0 & 0 & 0 & 0 \end{bmatrix} \tag{2.6}$$

$$\mathbf{K}=\begin{bmatrix} 0 & -R & Q & 0 & 0 & 0 & 0 & 0 & 0 \\ r & 0 & -P & 0 & 0 & 0 & 0 & 0 & 0 \\ -Q & P & 0 & 0 & 0 & 0 & 0 & 0 & 0 \\ 0 & -W & V & 0 & -R & Q & 0 & 0 & 0 \\ W & 0 & -U & R & 0 & -P & 0 & 0 & 0 \\ -V & U & 0 & -Q & P & 0 & 0 & 0 & 0 \\ 0 & 0 & 0 & 0 & 0 & 0 & 0 & 0 & 0 \\ 0 & 0 & 0 & 0 & 0 & 0 & 0 & 0 & 0 \\ 0 & 0 & 0 & 0 & 0 & 0 & 0 & 0 & 0 \end{bmatrix}$$

$$\mathbf{M}_s = f(\boldsymbol{V}, \boldsymbol{J}^1, \boldsymbol{S}^1)$$

$$\boldsymbol{Q} = [X, Y, Z, L, M, N, M_H, M_V, M_L]^\top$$

and

$\boldsymbol{V}$ – vector of velocity

$$\boldsymbol{V} = [U, V, W, P, Q, R, \dot{\delta}_H, \dot{\delta}_V, \dot{\delta}_L]^\top \tag{2.7}$$

$\mathsf{K}_{wz}\boldsymbol{H}$ – vector of constraint reactions

$$\mathsf{K}_{wz}\boldsymbol{H} = g(\Phi, \Theta, \Psi, P, Q, R, K^{H^1}, K^{V^1}, K^{L^1}) \tag{2.8}$$

J_i, J_i^1 and S_i, S_i^1 are the direct and modified inertia and static moments; K^i represents the modified gains (Graffstein et al., 1998; Maryniak, 1992).

Eq $(2.3)_1$ is supplemented by the kinematics relationships representing the general mathematical model of UAV (Graffstein et al., 1997; Maryniak, 1992), which was used in numerical simulation.

3. Numerical simulation of UAV recovery manoeuvre

Fig. 2. FOX AT in the recovery manoeuvre

Since the UAV is a device used many times it should be safely recovered after each mission by means of different landing techniques; i.e., classical landing gear (big UAV), landing skids and parachute. The latter one (Fig.2), however most complicated, was chosen for the UAV "SOWA" under analysis.

Numerical simulation of the recovery phase has been made, in which to the UAV recovery a parachute was applied launched at he initial velocity of

20 m/s. Fig.3 shows the pyrotechnic devices for launching constructed in the Institute of Aviation.

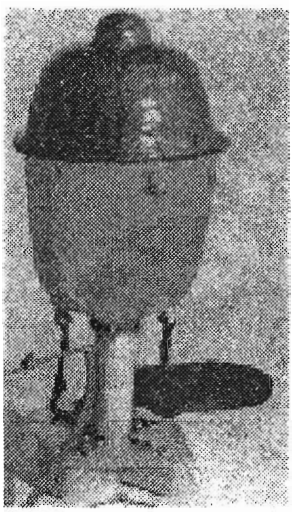

Fig. 3. Recovery system

There are two crucial elements in the recovery manoeuvre:

- minimisation of G-force
- assuring safe canopy deployment of a parachute (e.g. protection against entangling of the parachute lines a in rotating propeller).

This was attained by using special "sliders" in the UAV design, minimising the velocity of flight and ensuring that the UAV is suitable located relative to the opened canopy of parachute.

The UAV model represents also the effect of forces and moments that appear at the moments of cover opening and parachute launching.

In the considered case the assumption was accepted, that at the initial moment of the manoeuvre the UAV is in the specified horizontal flight, at the minimum velocity 32 m/s. At the beginning of the manoeuvre the thrust falls down (to zero) and the maximum elevator deflection does not exceed $\delta_H = 20°$ for very high values of the angle of pitch Θ to be attained (elevator deflection remains unchanged until the recover end). After the next 0.5 s the cover opens, and after another 0.5 s the parachute is launched (in Fig.6 and Fig.7 these events are represented by vertical lines).

The UAV and lunched parachute trajectories are shown in the inertial system $Ox_g y_g z_g$, (Fig.4 and Fig.5) which at the moment of parachute lunching

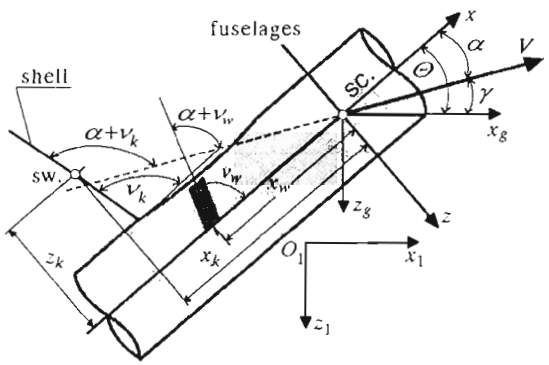

Fig. 4. Recovery system coordinates axes

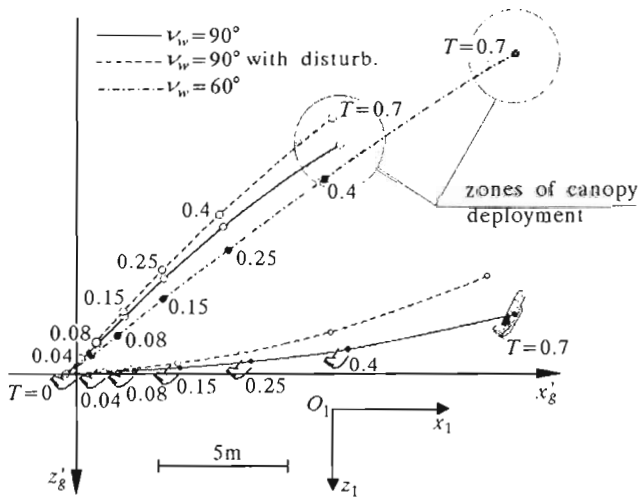

Fig. 5. Trajectory of the UAV and launched parachute

becomes fixed. For large increase in the pitch moment to be attained the cover angle of incidence was assumed to be 90°. The simulation was performed for the parachute lunching at the ν_w angles of 60° and 90°, respectively. The latter value was applied also under disturbance conditions at the horizontal 5 m/s gust of wind, directed opposite to the initial UAV direction of motion.

The following notations are used in presentation of the results of numerical simulation. In Fig.6 and Fig.7, the moments of cover opening and parachute lunching are represented by the vertical lines, the disturbance area is shown by thin vertical lines, while the grey area represents a hypothetical UAV state after the parachute canopy is opened (no parachute effect).

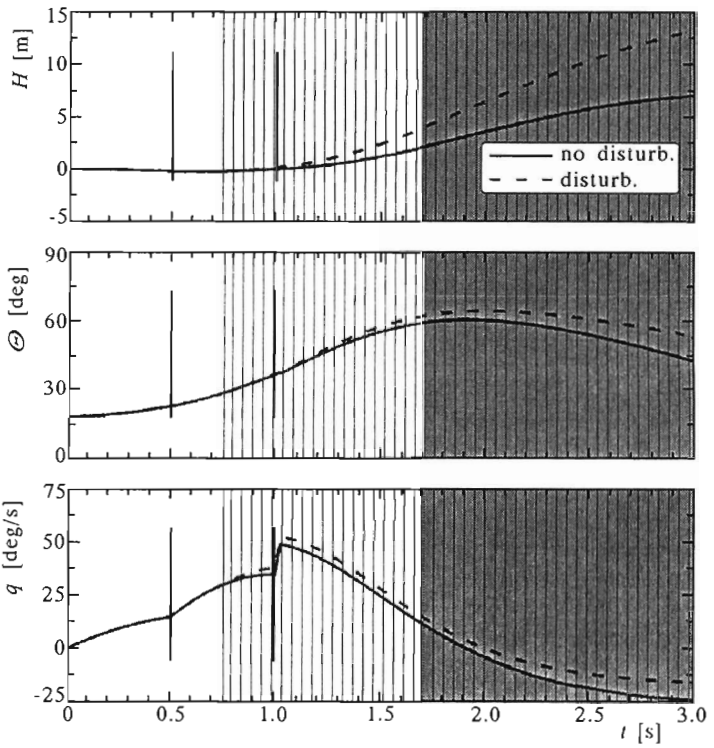

Fig. 6. Results of UAV recovery simulation

Changes in the pitch angle Θ (Fig.5 and Fig.6) result from the necessity for a suitable UAV location relative the parachute, at the moment the canopy is opened since a pitching moment due to the elevator deflection δ_H is positive. The two phases of recovery; i.e., cover opening and parachute lunching can be identified by analysing the changes in the course of pitch velocity Q shown in Fig.6, which is more difficult in the cases of angle of attack and velocity of flight V (Fig.7).

The angle ν of parachute lunching exerts essential influence on the simulated manoeuvre. From Fig.5 it can be seen that for $\nu_w = 60°$ the canopy deploys above UAV. Perhaps, it can bring about too high negative values of the pitching moment, however the increase in the angle ν_w up to $90°$ values eliminates practically this problem (Fig.5), also in the case of 5 m/s gust of wind disturbance.

As the pitch angle Θ and the angle of attack α decrease (Fig.6 and Fig.7), from the manoeuvre beginning total velocity of flight decreases substantially

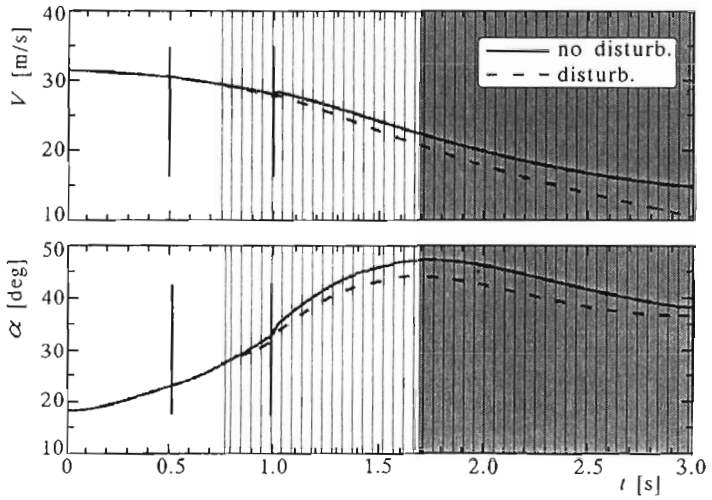

Fig. 7. Results of UAV recovery simulation

and at the moment of canopy deployment goes down to $V = 24\,\mathrm{m/s}$. From Fig.7 it can be seen that observed at the moment the UAV enters the area of critical angles of attack its velocity decreases below the critical values, which appear after the parachute launching.

4. Conclusions

From the results of numerical simulation presented in Fig.6 and Fig.7, we can conclude that the modelled UAV is practically completely resistant to disturbances having the form of gusts of wind.

The problem of UAV recovery is one of many complicated special manoeuvres, which have been worked out for the purposes of automati mission planning. The presented method is effective and worth recommendation for solving problems this type.

Acknowledgements

The research was supported by the State Committee for Scientific Research, under grants No. 0T00 A 036 17 and T12 C 06017.

References

1. BLAJER W., 1995, Uwagi o realizacji programowego ruchu samolotu po założonej trajektorii, *VI Konferencja Mechanika w Lotnictwie*, PTMTS, Warszawa, 19-31

2. BLAJER W., GRAFFSTEIN J., KRAWCZYK M., 1997, Aircraft Program Motion and Control in Prescribed Trajectory Flight, *IV Konferencja MMAR-97*, Międzyzdroje, 351-356

3. GRAFFSTEIN J., KRAWCZYK M., 1996, Presymulacja misji samolotu bezpilotowego, *II Konferencja Metody i technika badań statków powietrznych w locie*, Mrągowo, 42-47

4. GRAFFSTEIN J., KRAWCZYK M., MARYNIAK J., 1997, Modelowanie dynamiki lotu sterowanego autonomicznie samolotu bezpilotowego z wykorzystaniem teorii więzów nieholonomicznych, *XXXVI Sympozjon "Modelowanie w Mechanice", Zeszyty Naukowe Kat. Mech. Stos. Pol. Śląskiej*, **3**, 141-148

5. GRAFFSTEIN J., MARYNIAK J., KRAWCZYK M., 1998, Wpływ zaburzeń zewnętrznych na wyniki symulacji manewrów specjalnych samolotu bezpilotowego, *X Ogólnopolskie Sympozjum, "Symulacja Procesów Dynamicznych"*, Zakopane, 145-151

6. MARYNIAK J., 1992, Ogólny model matematyczny sterowanego samolotu, *V Konferencja Mechanika w Lotnictwie*, PTMTS, Warszawa, 575-592

Model matematyczny BSL w numerycznej symulacji manewru odzysku w locie zaburzonym

Streszczenie

W pracy przedstawiono model dynamiki lotu sterowanego samolotu bezpilotowego, który wyprowadzono posługując się formalizmem Boltzmanna-Hamela. Szeroko znane są problemy występujące podczas startu i odzysku tego rodzaju obiektów. Oba manewry charakteryzują się małą prędkością lotu, występowaniem dużych kątów natarcia oraz stosunkowo małą skutecznością sterowania, co powoduje konieczność opracowywania wyrafinowanych procedur pozwalających na bezpieczna realizacje tych faz lotu. W pracy zaprezentowano wyniki symulacji numerycznej początkowej fazy manewru odzysku, jaki opracowano dla samolotu bezpilotowego SOWA.

Manuscript received September 7, 1999; accepted for print October 7, 1999